Hydrol. Earth Syst. Sci. Discuss., doi:10.5194/hess-2016-386, 2016
Manuscript under review for journal Hydrol. Earth Syst. Sci.
Published: 1 August 2016

Hydrology and Earth System Sciences Discussions
Open Access

Effect of restoration vegetation on the stochasticity of soil erosion in a semi-arid environment

Ji Zhou [1,2,3], Bojie Fu [1,2,]* Guangyao Gao [1,2], Yihe Lü [1,2], Shuai Wang [1,2]

[1] State Key Laboratory of Urban and Regional Ecology, Research Center for Eco-Environmental Science, Chinese Academy of Science, Beijing 100085, PR China,

[2] Joint Center for Global Change Studies, Beijing 100875, PR China

[3] University of Chinese Academy of Sciences, Beijing 100049, PR China

*Corresponding author: Bojie Fu

E-mail: bfu@rcees.ac.cn

Address: State Key Laboratory of Urban and Regional Ecology, Research Center for Eco-Environmental Science, Chinese Academy of Science, P. O. Box 2871, Beijing 100085, PR China

Abstract:

The interaction between vegetation and soil erosion is a core problem in ecohydrological research. Although the effects of vegetation on soil erosion have been widely studied, the stochasticity of soil erosion in restoration vegetation types in water-limited environment is less investigated. Based on monitoring soil erosion over five rainy seasons, we employed probabilistic-trait analysis framework (OCIRS-Bayes) to assess the stochasticity of runoff and sediment generation in three typical restoration vegetation types (*Armeniaca sibirica* (T1), *Spiraea pubescens* (T2) and *Artemisia copria* (T3)) in the Loess Plateau of China, and applied binomial and Poisson distribution functions to predict the probability distribution of erosion random events. The results indicated that, in OCIRS-Bayes system, 130 rainfall events were subdivided into four types. Two types with relative high average precipitation (27.6 and 69.0 mm respectively) could cause larger probability of soil erosion in all vegetation types than other type with average precipitation being 5.0 mm. Under the same rainfall condition, T1 with largest crown structure have lowest average probability of runoff (23.1 %) and sediment (10 %) generation; T2 with thicker litter layer and denser root system have moderate runoff (34.6 %) and sediment (14.6 %) occurrence probability; the probability of runoff (34.6 %) and sediment (25.4 %) generating in T3 were relative higher. The probability distribution of numbers of times soil erosion events in all restoration vegetation could be well predicted by binominal and Poisson probabilistic models, however, parameter analysis implied that Poisson model is more suitable for predicting stochasticity of soil erosion over larger temporal scale. This study could be meaningful

Hydrol. Earth Syst. Sci. Discuss., doi:10.5194/hess-2016-386, 2016
Manuscript under review for journal Hydrol. Earth Syst. Sci.
Published: 1 August 2016

Hydrology and Earth System Sciences
Open Access
Discussions

to apply more effectively restoration on protecting the soil and water resources in the water-limited environment.

Key words: stochasticity, restoration vegetation, soil erosion, Poisson distribution,

1. Introduction

The climate change and anthropogenic activities accelerate soil erosion triggering soil deterioration, and degrading terrestrial ecosystem over worldwide (Marques et al., 2008;Portenga and Bierman, 2011). The stochasticity of soil erosion reflects the effect of environmental elements such as stochastic rainfall on the erosive variability (Kim. J et al., 2016). As one of important environment factors, vegetation plays an important role on disturbing the impact of rainfall on soil erosion. The interaction between plant and erosion processes is still a research frontier in ecohydrology (Ludwig et al., 2005;Rodr ǵuez-Iturbe et al., 2001). Actually, how plant affect the stochasticity of soil erosion implies the risk of erosion generation in complex natural conditions. Exploring the effect is meaningful to assessing the efficacy of soil control practices as well as corresponding ecosystem service in semi-arid regions (Fu et al., 2011).

The stochasticity approach based on probability theory is a crucial tool to describe the random phenomenon and their ecohydrologic effects in natural condition. Precipitation is one of most important source of environmental stochasticity to directly affect the uncertainty of soil erosion. As early as 1978, Eagleson, (1978) applied probabilistic-trait methods to simplify the randomness of rainfall event. He predicted the distribution of annual precipitation from observed storm sequences by Poisson and Gamma probability distribution functions. Due to the obvious disturbance of rainfall events on environment, especially on the water-limited condition, many hydrological responses which are closely related to rainfall has also expressed different randomness, and indicated by various probabilistic models. For instance, Verma et al, (2011) applied probabilistic methods to assess the influence of daily precipitation distribution on dynamic of soil moisture. Rodriguez-Iturbe et al, (1999) described the dynamics of soil moisture by probability distribution functions depending on water balance at point scale. Wang and Tartakovsky, (2011) employed probability density function to reduce the complexity of infiltration rate in heterogeneous soils. Additionally, the susceptibility of some disasters trigged by some extreme rainfall events—such as flood (Mouri et al., 2013), slope instability (Li et al., 2014), and landslide (Ya and Chi, 2011)—have also assessed by probabilistic models.

As to the soil erosion which is typical hydrological response of soil to rainfall, Moore, (2007) predicted runoff production through probability models of soil storage capacity, and Sidorchuk, (2005, 2009) combined the probabilistic and deterministic soil erosion components to analyze the stochasticity of interaction between soil structure and overflow during erosion process. These probabilistic-trait approaches closely related to the theory of water balance and some typical hydrological assumptions. This optimized the hydrological models to more precisely represent the randomness of hydrological responses, which could more effectively describe complex hydrological processes (Bhunya et al., 2007). However, under the framework of probability theory, there are still few studies to explore the probabilistic method to analyze the stochasticity of soil erosion. Especially, little effort has been made to systematically investigate how the signal of stochastic rainfall is transmitted to soil erosion in different restoration vegetation types based on observational data rather than on other model assumptions. In fact, this investigation deriving from specific experiment results probably have more practical meaning for understanding the stochastic interaction between rainfall and erosion.

Morphological structures of plant including canopy structure, root system, and litter layer formation were endowed with controlling-erosion functions (Gartner, 2007;Jost et al., 2012;Wang et al., 2012;Woods and Balfour, 2010). Due to these function, vegetation acts as an important role on reinfiltrating overland flow, storing runon and restructuring sediment fluxes (Ludwig et al., 2005;Moreno-de las Heras et al., 2010). This significantly restricts the capacity of surface flow for delivering erosive particle out of a soil-plant system during rainfall processes (Bautista et al., 2007;Puigdefábregas, 2005). How vegetation affects soil erosion was also further interpreted and predicted by some conceptual and empirical models (Kumar and Kushwaha, 2013;Mallick et al., 2014;Prasannakumar et al., 2011). Both of vegetation-driven-spatial-heterogeneity (VDSH) (Bautista et al., 2007) and trigger-transfer-reserve-pulse (TTRP) (Ludwig et al., 2005) conceptual frameworks have stressed the driving role of vegetation on controlling erosion. Wischmeier and Smith, (1978) defined the land use conditions as a factor in universal soil loss equation (USLE) to imply the importance of vegetation on predicting erosion module. However, the effect of vegetation on stochasticity of soil

Hydrol. Earth Syst. Sci. Discuss., doi:10.5194/hess-2016-386, 2016
Manuscript under review for journal Hydrol. Earth Syst. Sci.
Published: 1 August 2016

erosion was less studied. Theoretically, soil erosion generation triggered by the stochastic precipitation, indispensably expressed the randomness. This ubiquitous property in hydrological processes could also be affected by the hydrological function of plant. Therefore, the application of stochasticity method on analyzing the interaction between plant and soil erosion, could be meaningful to understand the mechanism of erosion generation as well as to improve the accuracy of prediction.

In this study, we monitored soil erosion in three typical restoration vegetation types over five years' rainy seasons in the Loess Plateau of China, and aim to (1) construct assessment frameworks to characterize the random events in stochastic environment, (2) investigate how the stochastic signal of rainfall transmit into soil erosion in different restoration vegetation types; and (3) assess the effect of probability modellings on predicting the stochasticity of soil erosion in vegetation types. By exploring the stochastic property of soil erosion from more comprehensive and objective aspects, this study could enrich the methodology of sensitivity analysis of soil erosion, and probably be meaningful for the selection of reasonable restoration vegetation for conserving the soil and water resources in the Loess Plateau, China.

2. Materials and methods

2.1 Study region description

The study was implemented in the Yangjuangou Catchment (36°42'N, 109°31'E, 2.02 km^2) which is located in the typical hilly-gully region of the Loess Plateau in China (Figure 1a). A semi-arid climate in this area is mainly affected by the North China

Hydrol. Earth Syst. Sci. Discuss., doi:10.5194/hess-2016-386, 2016
Manuscript under review for journal Hydrol. Earth Syst. Sci.
Published: 1 August 2016

monsoon. Annual average precipitation reaches approximately 533 mm, and the rainy season here spans from June to September (Liu et al., 2012). When the rainy season comes, some high-intensity precipitation more easily cause soil erosion as the Calcaric Cambisol (FAO-UNESCO, 1974) soil type has relative higher potential erodibility. Soil erosion was one of most environmental hazard and cause the ecosystem degradation in the Loess Plateau before 1980s (Wang et al., 2015). And after 1998, as a crucial soil and water resource protection project, the Grain-for-Green Project was widely implemented in the Loess Plateau. A large number of steeply sloped croplands were abandoned, restored or natural recovered by shrub and herbaceous plants(Cao et al., 2009;Jiao et al., 1999). And in the Yangjuangou Catchment, the main restoration vegetation distributed on hillslopes includes *Robinia. pseudoacacia Linn*, *Lespedeza davurica*, *Aspicilia fruticosa*, *Armeniaca sibirica*, *Spiraea pubescens*, and *Artemisia copria*, etc. All the restoration vegetation was planted over 20 years ago.

2.2 Experimental design and measurement

In the Yangjuangou Catchment, systematic long-term field monitoring experiments were conducted. We have mainly concentrated on the runoff production and sediment yield in designed runoff plots (Liu et al., 2012;Zhou et al., 2016), dynamic of soil moisture in different restoration vegetation (Wang et al., 2013;Zhou et al., 2015), and the ecosystem service assessment in the typical water-restricted environment (Fu et al., 2011). In this study, we monitored the soil erosion in three typical restoration vegetation (*Armeniaca sibirica* (T1), *Spiraea pubescens* (T2) and *Artemisia copria* (T3)) over five years' rainy seasons from 2008 to 2012 (figure 1b). Each restoration vegetation type was designed in three 3 m by 10 m closed runoff-plot all of which were distributed on southwest facing hillslopes with a 26.8% aspect. The boundaries of each runoff-plot were perpendicularly fenced by impervious polyvinylchloride (PVC) sheet with 50 cm depth. And a collection trough and storage bucket was installed at the bottom boundary to compose the collection-transmission system of runoff and sediment (Zhou et al., 2016). Two tipping bucket rain gauges were installed outside of runoff-plot to automatically record the precipitation with accuracy of 0.2mm. We counted the number of times of runoff and sediment generation in each runoff-plot based on natural precipitation stochastically generating in the experiment area over five rainy seasons. Meanwhile, we stored runoff and sediment in collection-transmission system, separated them after settling the collecting bottles for 24 hours, dried at 105℃over 8 hours and weighted. We further measured the field saturated hydraulic conductivity in three restoration vegetation types by Model 2800 K1 Guelph Permeameter (figure 1c) (Soilmoisture Equipment Corp,. Santa Barbara, CA, USA) to determine the infiltration capability of soil matrix. And visually estimated the restoration vegetation cover by thirty 1 m^2 quadrats distributed over each runoff-plot for 2-3 times over different periods of rainy season (figure 1d). At last, we measured the average height, crown width, leaf area index, and the thickness of litter layer in T1 to T3 (Bonham, 1989). More information was showed in table 1

Figure 1

Table 1

2.3 Analysis framework for erosion stochasticity

2.3.1 Construction of random events system

Each observed stochastic weather condition is defined as a random experiment. All the possible outcomes of a random experiment constitute a sample space (Ω) defined as observation random event (short for O event, the same as follow). O event is subdivided into two mutually exclusive random event types, one is rainfall random event (I event) and the other is non-rainfall random event (C event). Precipitation is a necessary condition of runoff production, therefore, the runoff production random event (R event) is a subset of I event. Similarly, R event is also a necessary condition of sediment migration random event (S event). As a result, S event is contained in R event. Above defined O, C, I, R, and S events could be regarded as five different elements constituting the OCIRS random events system which is a basic framework for quantifying environment stochasticity.

Precipitation is a crucial disturbance environmental factor to transmit their stochastic signals into the R and S events. Therefore, it is necessary to investigate and classify the characteristics of all I events. Firstly, the time interval between two adjacent individual I events is set to be more than 6 hours, which is a criteria for the classification of individual I event according to its duration. And secondly, considering the typical rainfall eigenvalues including precipitation, intensity and duration as well as the main rainfall patterns in the Loess Plateau (Wei et al., 2007), we used Ward's method of hierarchical cluster analysis to classify 130 individual I events into four types (figure 2c). They are I_A events with lowest average precipitation and intensity; I_B events with

Hydrol. Earth Syst. Sci. Discuss., doi:10.5194/hess-2016-386, 2016
Manuscript under review for journal Hydrol. Earth Syst. Sci.
Published: 1 August 2016

second largest average precipitation and intensity; I_C events whose average precipitation and duration are largest; and I_D event which was an individual extreme rainfall event. Table 2 summarizes the physical and probabilistic properties all the elements in OCIRS system. Finally, the whole confirming process of all elements in OCIRS system is sketched by figure 2a, and Venn diagrams in figure 2b explored the relationships of all elements in OCIRS. In fact, various combinations of I and C events formed different random event sequences which finally constituted the whole field monitoring period.

Figure 2

Table 2

2.3.2 Quantification of erosion stochasticity

In the sample space Ω, for each random event *E* which could be regarded as any elements of OCIRS system, we define *P(E)* as the proportion of time that *E* occurs in terms of relative frequency:

$$P(E) = \lim_{n \to \infty} \frac{n(E)}{n} = p_E \quad (1)$$

Theoretically, $n(E)$ is the number of times in n outcomes of observed random experiment that the event E occurs, and $p_E \in [0,1]$. Let I_m, m=1, 2, 3 and 4 be the I_A, I_B, I_C, and I_D which are mutually exclusive random event types composing I event. According to the law of total probability, the probability of R event *P(R)* is defined as follow:

Hydrol. Earth Syst. Sci. Discuss., doi:10.5194/hess-2016-386, 2016
Manuscript under review for journal Hydrol. Earth Syst. Sci.
Published: 1 August 2016

$$P(R) = P(RI) = P(R|\cup_{m=1}^{4} I_m)P(\cup_{m=1}^{4} I_m) = \sum_{m=1}^{4} P(R|I_m)P(I_m) = p_R \qquad (2)$$

And $P(R|I_m)$ is conditional probability that R event occur given that m^{th} I event type has occurred. Similarly, the probability of S event *P(S)* are showed as follow:

$$P(S) = P(SI) = P(S|\cup_{m=1}^{4} I_m)P(\cup_{m=1}^{4} I_m) = \sum_{m=1}^{4} P(S|I_m)P(I_m) = p_S \qquad (3)$$

Equation (2) and (3) quantify the effect of stochastic signal of rainfall on soil erosion. On the other hand, supposing an R or S event has occurred stochastically, based on Bayes formula, we furtherly deduces two equations as follow:

$$P(I_k|R) = \frac{P(I_kR)}{P(R)} = \frac{P(R|I_k)P(I_k)}{\sum_{m=1}^{4} P(R|I_m)P(I_m)} \qquad (4)$$

and

$$P(I_k|R) = \frac{P(I_kR)}{P(R)} = \frac{P(R|I_k)P(I_k)}{\sum_{m=1}^{4} P(R|I_m)P(I_m)} \qquad (5)$$

Equation (4) and (5) quantify how much the contributions of k^{th} type of I event on a R or S event stochastically generating at month or seasonal scale, which reflect the feedback of soil erosion to rainfall stochasticity. Equation (2)~(5) characterize the interaction of rainfall and erosion by means of probability theory and expression. Consequently, we designs the OCIRS-Bayes framework combining OCIRS system with Bayes method. It systematically describe the stochasticity of soil erosion in different restoration vegetation types through the monitoring experiment, which indicates the interaction of rainfall and soil erosion.

We defined X, Y as two discrete random variables which are real-valued functions defined on the sample space Ω. Let X, Y denote the numbers of times of R and S events occurrence respectively. And let another random variable Z assign the sample space Ω to z. $X(R) = x, Y(S) = y, Z(\Omega) = k, y \le x \le z$. *x*, *y*, *k* are integers. The ranges of X and Y are $R_X = \{all\ x: x = X(R), all\ R \in \Omega\}$ and $R_Y = \{all\ y: y = Y(S), all\ S \in \Omega\}$. The probability of x_i or y_j times of R or S events could be quantified by the probability mass function (PMF) as follow:

$$pmf_X(x_i) = P[\{R_i: X(R_i) = x_i,\ \ x_i \in R_X\}] \tag{6}$$

$$pmf_Y(y_j) = P\left[\left\{S_j: Y\left(S_j\right) = y_j,\ \ y_j \in R_Y\right\}\right] \text{ for } i \geq j \tag{7}$$

PMF in equation (6), (7) describe the general expression of probability distribution of all possible numbers of times of R or S events.

Actually, according to the property of Bernoulli experiment (Robert et al., 2013), the random variables X, Y obey binominal distribution. The PMF of X, and Y were defined as follow:

$$pmf_{Xbin}(x) = P_{Xbin}(X = x) = \begin{cases} \binom{n}{x} p_R^x (1 - p_R)^{n-x} & x = 0,1,2, \dots, n \\ 0 & elsewhere \end{cases} \tag{8}$$

and

$$pmf_{Ybin}(y) = P_{ybin}(Y = y) = \begin{cases} \binom{n}{y} p_S^y (1 - p_S)^{n-y} & y = 0,1,2, \dots, n \\ 0 & elsewhere \end{cases} \tag{9}$$

And the expectation and variance of X and Y are equation (10) and (11):

$$E_{Xbin}[X] = np_R,\ V_{Xbin}[X] = np_R(1 - p_R) \tag{10}$$

$$E_{Ybin}[Y] = np_S,\ V_{Ybin}[Y] = np_S(1 - p_S) \tag{11}$$

where x and y indicate all possible numbers of times of R and S occurring over n independent I events which are also characterized as n Bernoulli experiments. However, when the Bernoulli experiment is performed infinite independent times ($n \rightarrow \infty$), the binomial PMF can be transformed into Poisson PMF, which is proved by appendix A. Therefore, equation (8) and (9) can be transformed as follow:

$$pmf_{Xpoi}(x) = P_{Xpoi}(X = x) = \begin{cases} \frac{\lambda_R^x e^{-\lambda_R}}{x!} & x = 0,1,2,\dots \\ 0 & elsewhere \end{cases} \tag{12}$$

and

$$pmf_{Ypoi}(y) = P_{Ypoi}(Y = y) = \begin{cases} \frac{\lambda_S^y e^{-\lambda_S}}{y!} & y = 0,1,2,\dots \\ 0 & elsewhere \end{cases} \tag{13}$$

And expectation and variance of X and Y are :

$$E_{Xpoi}[X] = V_{Xpoi}[X] = \lambda_R \tag{14}$$

$$E_{Ypoi}[Y] = V_{Ypoi}[Y] = \lambda_S \tag{15}$$

where the parameter $\lambda_R \approx np_R, \lambda_S \approx np_S$. As a result, equation (8)~(11) reflect two PMF models to construct the prediction system of stochasticity of soil erosion.

2.4 Statistics

We employed nonparametric statistical tests—one-way ANOVA and post hoc LSD—to determine the significant difference of soil, vegetation and erosive properties in the three restoration vegetation types, and took Spearman's rank correlation coefficients to analyze how the vegetation coverage affect the probability of soil erosion generation under three grouped precipitation types. At last, the maximum likelihood estimator (MLE) and uniformly minimum variance unbiased estimator (UMVUE) (Robert et al., 2013) were explored to compare the suitability of the binomial PMF and Poisson PMF for predicting the uncertainty of runoff and sediment generation over long term.

3. Results

3.1 Stochasticity of classified rainfall

The stochasticity of I event in OCIRS system is a direct source of randomness of soil erosion. According to cluster analysis, all I events were classified into four categories including I_A, I_B, I_C and I_D (figure 2c). Firstly, I_A type was characterized as lowest average precipitation (5 mm), intensity (0.015 mm/min) and duration (365 minutes) in the four categories types. The proportion of I_A to all I events reaches to 72% with its higher reoccurrence in each rainy seasons (figure 3). Especially, in 2010, nearly 90% of I events was I_A. However, due to its small rainfall erosivity, the times of R and S events occurring in three vegetation restoration types was lowest under I_A condition (table 3). Secondly, characterized as high average rainfall intensity (0.072 mm/min), I_B event has the second higher occurrence probability in each rainy season (figure 3). Even in 2008, the proportion of I_B to all I events (50%) was larger than that of I_A (33%). Although the average probability of I_B event occurrence approximated to 5% in all O events of five rainy seasons, I_B can more easily lead to soil erosion in three restoration vegetation types. Especially, when each I_B event occurred stochastically in five rainy seasons, then it would nearly trigger R event in type 2 and 3 restoration vegetation (table 3). Thirdly, the probability of I_C event with highest average precipitation (69 mm) occurring in each rainy season is 1% in all O events of five rainy seasons. In the rainy season of 2010, there was even no I_C occurrence. However, if each I_C event stochastically generated in rainy seasons, the R event would occurred in all restoration vegetation types. On July, 2008, there was a specific I event with extreme high rainfall intensity (0.78 mm/min) which was classified I_D event. I_D event was very rare, because it was observed one times over five rainy seasons. Under this precipitation condition, soil erosion generated in all restoration vegetation types.

Figure 3

Table 3

3.2 Stochasticity of soil erosion in vegetation types

Based on OCIRS system, the stochasticity of soil erosion in three restoration vegetation types (T1, T2 and T3) at month and seasonal scales is described by figure 4. At early period of erosion monitoring, the stochasticity of soil erosion in all restoration vegetation types is similar, with probability of R and S event generation ranging from 6% to 13% and from 3% to 13% respectively. From rainy season of 2009 to 2011, the highest probabilities of soil erosion in each vegetation type all appeared in the middle of rainy season (July and August). However, these probabilities were observed to be different extents of decrease with the increasing of experiment period. As to runoff production, the probability of R event generation in T1 was generally less than that of T2 and T3 under same precipitation condition, with it being less than 7% in the last four rainy seasons. The randomness of R events occurring in T2 and T3 have similar distribution in each month of rainy season. With respect to sediment yield, the probability reduction of S event generating in T1 was more obvious than that of other types, with it being only less than 3% in the last four rainy seasons. Especially, in the rainy season of 2011 and 2012, there was no S event occurrence in T1, however, the corresponding average probability of S event in T2 and T3 was near 1.5% and 4% respectively. Generally, influenced by the same stochastic signal of I events, T1 and T3 have the lowest and highest probability of soil erosion respectively.

According to the Bayes formula, figure 5 indicated that given one R or S event has stochastically generated in some restoration vegetation type at specific month or rainy season, how much the probabilistic contribution of different types of I events on the corresponding soil erosion occurrence. In the rainy season of 2008, as to all restoration vegetation types, the contributing types of I events on soil erosion was more complex than other rainy seasons, but also concentrated on relative high precipitation and intensity classified I events such as I_B, I_C events. With the increasing of experiment duration from 2009 to 2011, the complexity seemed to be reduced, and the probabilistic contribution of I_A event on soil erosion have different extent increase in three restoration vegetation types. If one R event has stochastically occurred in T1, the probabilistic contribution on this runoff production were generally I_B and I_C events, which they ranged from about 50% to 100% and near 20% to100% respectively. And I_A and I_B events have even no probabilistic contribution on one S event occurring on T1 stochastically over the last four rainy seasons. However, I_A and I_B events have been the main probabilistic contributors for one statistical soil erosion generation on T2 and T3, which they ranged from about 10% to 100% and 30% to 100% respectively. Consequently, the contribution pattern of I events on soil erosion in T1 was relative simple and mainly focused on I events type with higher rainfall erosivity than that of in

Hydrol. Earth Syst. Sci. Discuss., doi:10.5194/hess-2016-386, 2016
Manuscript under review for journal Hydrol. Earth Syst. Sci.
Published: 1 August 2016

T2 and T3.

Figure 4

Figure 5

3.3 Prediction of soil erosion stochasticity

We defined ten consecutive stochastic I events as an stochastic environment unit of the background of soil erosion, which indicates that n =10 in the binomial and Poisson distribution functions (equation (8~9, 12~13)). Under this assumption, figure 6 describes binomial and Poisson PMFs to predict the probability distributions of numbers of times of soil erosion events in three restoration vegetation types. It also compares the predictions with the frequencies of numbers of times of observed R and S event in vegetation types. Firstly, as to the probability distribution of R event, it seems that the binomial and Poisson PMFs provide a better fit to the observation in T1 than that of in T2 and T3. More specifically, in all restoration vegetation types, binomial PMFs supply better fit to the observed numbers of time of R events with larger frequency (such as 2~4 time) than that of Poisson PMFs. However, Poisson PMFs fit the observed numbers of time of R events with the lower frequency (such as 6~8 times) better than that of binomial PMFs. The frequencies of observed numbers of time of R events in T2 and T3 have similar distribution patterns. Secondly, with respect to probability distribution of S event, the predictions about the observed probability distribution of S events in T1 by both PMFs do not fit very well. Especially, when the frequency of number of times of no-sediment in T1 is nearly two times larger than the corresponding predication of binomial and Poisson PMFs. However, the two PMFs are seemed to provide better fit to the observation in T3 and T2 than that of in T1. With the restoration vegetation types changing from T1 to T3 in figure 6, the predicted or observed numbers of time of R events with largest probability or frequency increased in consistence. Generally, Poisson PMF seems to provide better probability distribution prediction about observed numbers of times of R events in all restoration vegetation types than that of Binomial PMF.

Figure 6

4. Discussion

4.1 OCIRS-Bayes framework for erosion stochasticity

The OCIRS designing and Bayes method in this paper constitute an innovative analysis framework for soil erosion study. Environmental stochasticity is an inevitable factors to affect the variability of soil erosion, which is also a non-negligible obstacle for the understanding of soil erosion and its modelling prediction (Kim. J et al., 2016). OCIRS-Bayes framework formed a random event system to evaluate the stochasticity of environment, but also analyze the transmission of stochastic signal of rainfall into soil erosion. In this framework, the stochastic weather conditions were defined as a series random events with various physical and probabilistic meanings, which have direct or indirect relevance to stochasticity of soil erosion (table 2). There also exist many modelling systems to evaluate the effect of influencing factors on soil erosion, and universal soil loss equation (USLE) is a typical one which models intensity of influencing factors to be predicted the erosion module by empirical formula (Wischmeier and Smith, 1978). But, there are less analysis frameworks like OCIRS-Bayes to model the stochasticity of soil erosion and its influencing factors totally depending on the long-term experimental data and fundamental probability theories. In order to stressed that the stochastic signals of rainfall events are the most important disturbances and sources of uncertainty and variability of soil erosion, OCIRS-Bayes further subdivides all rainfall events into various subsets (from I_A to I_D event) representing different rainfall erosivities which was similar with the typical rainfall patterns in rainy seasons of the Loess Plateau (Wei et al., 2007). Therefore, OCIRS-Bayes become a more practicable and simplification system to supplement to the studies on evaluating effect of rainfall properties on soil erosion in semi-arid environment.

In this study, OCIRS-Bayes framework discovered that the probability of soil erosion is closely related to the complexity of rainfall event types distributing in rainy season, which affected by the transmission of stochastic signals of high-erosivity rainfall events (such as I_C and I_D). This systematically analyzed how the stochastic signals of different rainfall events transmits to the soil erosion in restoration vegetation types in the water-limited natural condition at different temporal scales (showed in figure 4). Meanwhile, this framework also explored that the only relative high-erosivity rainfall events can make a contribution for the stochastically soil erosion generating in T1, which implied

Hydrol. Earth Syst. Sci. Discuss., doi:10.5194/hess-2016-386, 2016
Manuscript under review for journal Hydrol. Earth Syst. Sci.
Published: 1 August 2016

Hydrology and Earth System Sciences
Open Access
Discussions

the feedback of rainfall properties to stochasticity of soil erosion. Therefore, the interactive relationship between rainfall and soil erosion under restoration vegetation condition was characterized by OCIRS-Bayes framework. This supplies a new and meaningful aspect to understanding the soil erosion properties especially under the background of climate change transmitting more stochastic and extreme environmental signals into soil-plant system.

4.2 Disturbances of vegetation on erosion stochasticity

The different stochasticity of soil erosion in three restoration vegetation types reflects the different extents of disturbance of vegetation types on the transmission of stochastic signals of rainfall into soil-plant systems. These disturbances is closely related to the variety of morphological structure with complex ecohydrological functions affecting the whole process of runoff production and sediment yield (Jost et al., 2012; Wang et al., 2012; Woods and Balfour, 2010). Specifically, the morphological structures including canopy, litter layer and root distribution could have obvious hydrological function to control soil erosion. Firstly, the largest crown diameters of T1 could have stronger interception capacity than that of T2 and T3. Because many studies have proved that canopy structure could have specific capacities for precipitation retention, and prevent rainfall from directly forming overland flow or splashing soil surface particles (Liu, 2001;Mohammad and Adam, 2010;Morgan, 2001), For this reason, the canopy structure of T1 could have stronger capacity to reduce the transmission of stochastic signal of amount and energy of rainfall directly on soil surface, which finally

Hydrol. Earth Syst. Sci. Discuss., doi:10.5194/hess-2016-386, 2016
Manuscript under review for journal Hydrol. Earth Syst. Sci.
Published: 1 August 2016

Hydrology and Earth System Sciences
Open Access
Discussions

attributed to the relative lower probability of R and S event in T1. This could also probable explained the decreased vegetation coverage significantly correlated with the increased probability of S event in table 4.

Secondly, there was abundant litter material covering on the soil surface of T2 (figure 7), which formed a significant largest average thickness of the litter layer. Many studies also proved that litter layer structure acts multiple roles on conserving the rainfall, improving infiltration of throughfall, as well as cushioning the splashing of raindrop (Gyssels et al., 2005;Johns, 1983;Munoz-Robles et al., 2011;Geißler et al., 2012). For these reasons, the litter layer structure of T2 also have stronger disturbance on the transmission of stochastic signals of rainfall through improving the throughfall absorption to reduce the probability of R event as well as inhibiting the splash or sheet erosion occurrence.

The distribution of root system could be the third important morphological structure to disturb the stochastic signal of rainfall transmitting on soil-plant system. More macropores formed by root system of vegetation types distributing in the soil matrix was proved to improve the reinfiltration of the overland (Gyssels et al., 2005). The reinfiltration process is an important way to recharge soil water stores when the overland flow occurred in hillslopes, but also an indispensable contributing factor to reduce the unit area runoff (Moreno-de las Heras et al., 2009;Moreno-de las Heras et al., 2010). Consequently, showed in figure 7, denser root system distributing the underground of T2 could create more macropores in the subsurface than that of T1 and T3. It reduce the transmission of stochastic signal of rainfall by means of supplying more opportunity to reinfiltrate the potential overland flow into a deep soil layer, and finally decreased the probability of soil erosion in T2.

The interactions between plant and soil erosion in semi-arid environment is a complex ecohydrological processes (Ludwig et al., 2005), which also reflects in the complexity of stochasticity of soil erosion in different restoration vegetation types. However, due to the mechanical characteristics of morphological structures of vegetation having strong negative correlation with soil erosion in this study region (Zhu et al., 2015), these hydrological-trait morphological structures of vegetation could be key factors to affect the randomness of soil erosion. Just as in this study, the limited hydrological-trait morphological structures—such as relative smaller canopy structure, thinner thickness of litter layer, and shallower root system distribution in soil layer of T3—more significantly restricted its hydrological functions on intercepting rainfall as well as on conserving overland flow than that of T1 and T2 with obvious canopy structure and thicker litter respectively. As a result, these differences of morphological structures finally lead to the different stochasticity of runoff and sediment in T1 to T3.

Figure 7

Table 4

4.3 Assessment of stochasticity prediction modellings

PMFs of binomial and Poisson are effective probabilistic modellings to predict the stochasticity of soil erosion in restoration vegetation types in semi-arid environment.

Hydrol. Earth Syst. Sci. Discuss., doi:10.5194/hess-2016-386, 2016
Manuscript under review for journal Hydrol. Earth Syst. Sci.
Published: 1 August 2016

The binomial and Poisson distribution functions were extensively applied on analyzing the stochastic hydrological phenomenon in natural condition Eagleson (1978). In the OCIRS-Bayes analysis framework, R and S events were both subsets of sample space composed by I events, therefore, the stochasticity of R and S have close connection with the stochastic signals of I events. In this study, the PMFs of binomial and Poisson indicates relative good predication about probabilistic distribution of soil erosion in all restoration vegetation types over five rainy seasons, however, with the ongoing experiment (supposing the monitoring of soil erosion last for 10 rainy seasons' for instance), whether these two PMFs would still have stable and consistent well-prediction about the stochasticity of soil erosion in T1 to T3, which could be an interesting and important assessment of the two PMFs. Based on above assumption, we compared the temporal effects of prediction in the two PMFs, and employed MLE and UMVUE (Robert et al., 2013) which are most important point estimation methods to make parameter analysis on PMFs of binomial and Poisson. The parameters p_R, p_S, λ_S and λ_R are deduced from experimental data, and contain all stochasticity information about R and S occurring in different restoration vegetation types. Specifically, take the stochasticity of R event for instance, we defined X_i as the number of times of R event occurrence in a specific restoration vegetation in i th rainy season. Therefore, in this study, five independent and identical (*iid*) random variables have the same and mutually independent PMFs of binomial or Poisson, which are simply expressed as follow:

$$\mathrm{X}_1, \mathrm{X}_2, \ldots, \mathrm{X}_5 \overset{iid}{\rightarrow} binomial\ (p_R) \text{ or } \mathrm{X}_1, \mathrm{X}_2, \ldots, \mathrm{X}_5 \overset{iid}{\rightarrow} Poisson\ (\lambda_R) \tag{16}$$

Supposing the monitoring of soil erosion are continued to be conducted infinitely, then the numbers of corresponding I events (n) and rainy seasons (i) would approach infinity (n, $i \to \infty$). (16) would be transformed as follow:

$$\mathrm{X}_1, \mathrm{X}_2, \ldots, \mathrm{X}_i \xrightarrow{iid} binomial\ (p) \text{ or } \mathrm{X}_1, \mathrm{X}_2, \ldots, \mathrm{X}_i \xrightarrow{iid} Poisson\ (\lambda) \qquad (17)$$

In the (17), p and λ are two population parameters representing the whole randomness information of R events under longer monitoring period with i rainy seasons. The real p or λ is unknown, but, theoretically, they can be estimated by searching for the best reasonable population estimators $\hat{p}$ or $\hat{\lambda}$ through MLE and UMVUE methods. During the estimator searching processes, appendix B proved that the best estimator $\hat{p}$ in Binomial PMF is the unbiasedness and consistency of the MLE of p. And appendix C, however, proved that the best estimator $\hat{\lambda}$ in Poisson PMF is not only the unbiasedness and consistency of the MLE of λ, but also the UMVUE of MLE. Consequently, comparing the two appendices, the best estimator $\hat{\lambda}$ implies that the Poisson PMF would be more beneficial for predicting the stochasticity of R and S events in different restoration vegetation types over long-term observation periods than that of Binomial PMF.

Besides having better prediction about stochasticity of soil erosion at larger temporal scale, the Poisson PMF could also be fit for predicting the stochasticity of S event in the closed-design plot system. As Boix-Fayos et al, (2006) mentioned, the closed runoff-plot was not fit for long-term soil erosion monitoring, because it forms an obstruction to prevent the transportable material from entering the close monitoring system. With the ongoing monitoring at longer temporal scale, the transport-limited erosion pattern could gradually transform into detachment-limited pattern in the closed-

Hydrol. Earth Syst. Sci. Discuss., doi:10.5194/hess-2016-386, 2016
Manuscript under review for journal Hydrol. Earth Syst. Sci.
Published: 1 August 2016

plot (Boix-Fayos et al., 2007;Cammerraat, 2002). This probably leads to the sediment transformation becoming more and more difficult to generate, and finally reduces the probability of S events under the same precipitation condition. And fortunately, the parameters in Poisson PMF at larger temporal scale could successfully express the decreasing of probability of S event in closed-plot system. Because, in order to satisfying the fact that $\lambda = np$ in Poisson PMF is an unknown constant, when the numbers of times of I events (n) approach infinity, the probability (p) of R or S events generation have to approach to zero, Actually, above inference coincides with the assuming situation for sediment transformation in closed plot system at long temporal scale (Boix-Fayos et al., 2006), which further proves that Poisson PMF could be a reliable prediction model for soil erosion. However, affected by the globe climate change, the occurring frequency of extreme weather condition probably increase. Under that background, the stochastic signals of increasing extreme I events could inevitably be transmitted into the stochasticity of soil erosion in the further. Consequently, it is necessary to furtherly focus on the disturbance of rare event with extreme amount or energy on the soil-plant systems under a changing environment.

5. Conclusion

In this study, we applied stochastic approach to analyze the effects of restoration vegetation types on the stochasticity of runoff and sediment in the Loess Plateau of China, and draw the following conclusions:

(1) OCIRS-Bayes framework is an innovative analysis system which not only quantify

Hydrol. Earth Syst. Sci. Discuss., doi:10.5194/hess-2016-386, 2016
Manuscript under review for journal Hydrol. Earth Syst. Sci.
Published: 1 August 2016

Hydrology and Earth System Sciences
Open Access
Discussions

the stochasticity of environment in terms of random event pattern, but also characterize the interactive relationship between rainfall and soil erosion by means of probability theory.

(2) The difference of morphological structures in restoration vegetation types is the source of different stochasticity of soil erosion in T1 to T3 under same rainfall condition. Larger canopy, thicker litter layer and denser root distribution could more effectively affect the transmission of stochastic signal of rainfall into soil erosion.

(3) Both of binomial and Poisson PMFs could well predict the probability distribution of numbers of times runoff and sediment events in T1 to T3, however, Poisson PFM could be more fit for predicting stochasticity of soil erosion at larger temporal scales

This study provide a new analysis framework to describe the soil erosion property, which could be meaningful to researchers and policy makers to evaluate the efficacy of soil control practices and their ecosystem service in a semi-arid environment.

Appendix A. The transformation from binominal to Poisson PMF

Let $p = \frac{\lambda}{n}$, then:

$$pmf_{Xbin}(x) = \binom{n}{x} p^x (1-p)^{n-x} = \frac{n!}{x!(n-x)!} \cdot \left(\frac{\lambda}{n}\right)^x \cdot \left(1-\frac{\lambda}{n}\right)^{n-x}$$

$$= \frac{\lambda!}{x!} \cdot \frac{n(n-1)(n-2)\cdots 1}{(n-x)(n-x-1)\cdots 1} \cdot \frac{1}{n^x} \cdot \left(1-\frac{\lambda}{n}\right)^{n-x}$$

$$= \frac{\lambda!}{x!} \cdot 1 \cdot \left(1-\frac{1}{n}\right) \cdot \left(1-\frac{2}{n}\right) \cdots \left(1-\frac{x-1}{n}\right) \cdot \left(1+\frac{-\lambda}{n}\right)^n \cdot \left(1-\frac{\lambda}{n}\right)^{-x} \qquad \text{(A1)}$$

Hydrol. Earth Syst. Sci. Discuss., doi:10.5194/hess-2016-386, 2016
Manuscript under review for journal Hydrol. Earth Syst. Sci.
Published: 1 August 2016

Hydrology and Earth System Sciences Open Access Discussions

In equation (A1), when $n \to \infty$, and x, λ is finite and constant, then

$$\lim_{n\to\infty}(1-\frac{1}{n}) = \cdots = \lim_{n\to\infty}\left(1-\frac{x-1}{n}\right) = \lim_{n\to\infty}\left(1-\frac{\lambda}{n}\right)^{-x} = 1 \tag{A2}$$

And

$$\lim_{n\to\infty}\left(1+\frac{-\lambda}{n}\right)^{n} = e^{-\lambda} \tag{A3}$$

And according to equation (A2) and (A3), the equation (A1) can be transformed as:

$$\lim_{n\to\infty}\left[\frac{n!}{x!\,(n-x)!}\cdot\left(\frac{\lambda}{n}\right)^{x}\cdot\left(1-\frac{\lambda}{n}\right)^{n-x}\right] = \frac{\lambda^{x}e^{-\lambda}}{x!} \quad x = 0,1,2,\ldots \tag{A4}$$

or

$$pmf_{Xbin}(x)\xrightarrow{n\to\infty}\frac{\lambda^{x}e^{-\lambda}}{x!} = pmf_{Xpoi}(x) \tag{A5}$$

Appendix B. Parameter estimation of p in Poisson PMF

(1) Derivatization of the MLE $\hat{p}$

Let the random sample $\mathrm{X}_1, \mathrm{X}_2, \ldots, \mathrm{X}_i \overset{iid}{\rightarrow} pmf_{Xbin}(p)$ and assume the binomial distribution as:

$$P(\mathrm{X}=x_i) = \binom{m}{x_i}p^{x_i}(1-p)^{m-x_i} \tag{B1}$$

The likelihood function $L(p)$ is joint binomial PDF with parameter p as follow:

$$L(p) = f_X(\mathrm{X}_1,\ldots,\mathrm{X}_n,p) = \prod_{i=1}^{n}\binom{m}{x_i}p^{\sum_{i=1}^{n}\mathrm{X}_i}(1-p)^{(mn-\sum_{i=1}^{n}\mathrm{X}_i)} \tag{B2}$$

By taking logs on both side of equation (B2):

$$lnL(p) = ln\left(\prod_{i=1}^{n}\binom{m}{x_i}\right) + \sum\nolimits_{i=1}^{n}\mathrm{X}_i\, ln\, p + \left(mn - \sum\nolimits_{i=1}^{n}\mathrm{X}_i\right) ln(1-p) \tag{B3}$$

And differentiating with respect to p in $lnL(P)$ and let the result be zero:

$$\frac{\partial lnL(p)}{\partial p} = \frac{\sum_{i=1}^{n}\mathrm{X}_i}{p} - \frac{(mn-\sum_{i=1}^{n}\mathrm{X}_i)}{(1-p)} = 0 \tag{B4}$$

Solution $\hat{p} = \frac{\sum_{i=1}^{n}\mathrm{X}_i}{mn}$, let $m = n, \Longrightarrow \hat{p} = \frac{\bar{\mathrm{X}}}{n}$

Hydrol. Earth Syst. Sci. Discuss., doi:10.5194/hess-2016-386, 2016
Manuscript under review for journal Hydrol. Earth Syst. Sci.
Published: 1 August 2016

Hydrology and Earth System Sciences
Discussions
Open Access

Therefore, $\hat{p} = \frac{\overline{X}}{n}$ is the MLE of population parameter p in binomial PMF model.

(2) Discussion of the unbiasedness and consistency of $\hat{p}$

Let $E_p(\hat{p})$ be the expectation of M.L.E $\hat{p}$ when population parameter p is true in random sample which is $X_1, X_2, \dots, X_i \xrightarrow{iid} pmf_{Xbin}(p)$, then

$$E_p(\hat{p}) = E_P(\overline{X}/n) = \frac{1}{n^2}\sum_{i=1}^{n} E_P(X_i) = \frac{1}{n^2}n^2 p = p \tag{B5}$$

Which proved that MLE $\hat{p} = \frac{\overline{X}}{n}$ is a unbiased estimator for p. And furthermore then let $Var_p(\hat{p})$ be the variance of $\hat{p}$ when population p is true.

$$Var_p(\hat{p}) = Var_p\left(\sum_{i=1}^{n} X_i/n^2\right) = \frac{1}{n^4}\sum_{i=1}^{n} Var_p(X_i) = \frac{p(1-p)}{n^2} \tag{B6}$$

As the n approaches to infinite:

$$\lim_{n\to\infty} Var_p(\hat{p}) = \lim_{n\to\infty}\left(\frac{p(1-p)}{n^2}\right) = 0 \tag{B7}$$

Equation (B5)~(B7) satisfied the theme of weak law of larger number, which lead the $\hat{p} = \frac{\overline{X}}{n}$ is probabilistic converge to population parameter p:

$$\lim_{n\to\infty} P(|\hat{p} - p| \geq \varepsilon) = 0, \text{for all } \varepsilon > 0 \tag{B8}$$

Consequently, the unbiased MLE $\hat{p} = \frac{\overline{X}}{n}$ is consistent for p.

Appendix C. Parameter estimation of λ in Poisson PMF

(1) Derivatization of the MLE $\hat{\lambda}$

Let the random sample $X_1, X_2, \dots, X_i \xrightarrow{iid} pmf_{Xpoi}(\lambda)$, and assume the poisson distribution as:

$$pmf_{Xpoi}(x_i) = \frac{\lambda^{x_i} e^{-\lambda}}{x_i!} \tag{C1}$$

Hydrol. Earth Syst. Sci. Discuss., doi:10.5194/hess-2016-386, 2016
Manuscript under review for journal Hydrol. Earth Syst. Sci.
Published: 1 August 2016

The likelihood function $L(\lambda)$ is joint PDF with parameter λ as follow:

$$L(\lambda) = f_X(\mathrm{X}_1, \dots, \mathrm{X}_n, \lambda) = f(\mathrm{X}_1, \lambda) \times \cdots \times f(\mathrm{X}_n, \lambda) = \prod_{i=1}^{n} \frac{\lambda^{x_i} e^{-\lambda}}{x_i!} \qquad \text{(C2)}$$

Taking logs on $L(\lambda)$ in equation (B4) and differentiating logarithm function with respect to λ:

$$\frac{\partial lnL(\lambda)}{\partial \lambda} = \frac{\partial\left(\prod_{i=1}^{n} \frac{\lambda^{x_i} e^{-\lambda}}{x_i!}\right)}{\partial \lambda} = -n \frac{\lambda^{\sum_{i=1}^{n} \mathrm{X}_i}}{(x_1 x_2 \cdots x_n)!} e^{-n\lambda} + \frac{\sum_{i=1}^{n} \mathrm{X}_i \lambda^{\left(-1+\sum_{i=1}^{n} \mathrm{X}_i\right)}}{(x_1 x_2 \cdots x_n)!} \qquad \text{(C3)}$$

Let the equation (C3) equal to zero, and has solution:

$$\hat{\lambda} = \frac{1}{n} \sum_{i=1}^{n} \mathrm{X}_i = \overline{\mathrm{X}} \qquad \text{(C4)}$$

Therefore, $\hat{\lambda} = \overline{\mathrm{X}}$ is the MLE of population parameter λ in Poisson PMF model.

(2) Discussion of the unbiasedness and consistency of $\hat{\boldsymbol{\lambda}}$

Let $E_\lambda(\hat{\lambda})$ be the expectation of MLE $\hat{\lambda}$ when population parameter λ is true in random sample $\mathrm{X}_1, \mathrm{X}_2, \dots, \mathrm{X}_i \overset{iid}{\rightarrow} pmf_{\mathrm{X}poi}(\lambda)$, then:

$$E_\lambda(\hat{\lambda}) = E_\lambda(\overline{\mathrm{X}}) = \frac{1}{n^2} \sum_{i=1}^{n} E_\lambda(\mathrm{X}_i) = \frac{1}{n} n\lambda = \lambda \qquad \text{(C5)}$$

which proved that MLE $\hat{\lambda} = \overline{\mathrm{X}}$ is a unbiased estimator for λ. Meanwhile, let $Var_\lambda(\hat{\lambda})$ be the variance of MLE $\hat{\lambda}$ when population parameter λ is true

$$Var_\lambda(\hat{\lambda}) = Var_\lambda(\overline{\mathrm{X}}) = Var_\lambda\left(\sum_{i=1}^{n} \mathrm{X}_i / n^2\right) = \frac{1}{n^4} \sum_{i=1}^{n} Var_\lambda(\mathrm{X}_i) = \frac{\lambda}{n} \qquad \text{(C6)}$$

And

$$\lim_{n\to\infty} Var_\lambda(\hat{\lambda}) = \lim_{n\to\infty} \left(\frac{\lambda}{n}\right) = 0 \qquad \text{(C7)}$$

According to the weak law of large number theme, equation (B7, B8, C1) lead that unbiased MLE $\hat{\lambda} = \overline{\mathrm{X}}$ is probabilistic converge to λ:

$$\lim_{n\to\infty} P\left(\left|\hat{\lambda} - \lambda\right| \geq \varepsilon\right) = 0, \text{for all } \varepsilon > 0 \qquad \text{(C8)}$$

Hydrol. Earth Syst. Sci. Discuss., doi:10.5194/hess-2016-386, 2016
Manuscript under review for journal Hydrol. Earth Syst. Sci.
Published: 1 August 2016

Therefore, MLE $\hat{\lambda} = \overline{\mathrm{X}}$ is consistent for population parameter λ.

(3) Determination of UMVUE $\hat{\lambda}$ of population parameter

Firstly, MLE $\hat{\lambda} = \overline{\mathrm{X}}$ is an unbiased estimator of parameter λ which is the precondition of UMVUE determination. Secondly, by using Cramer-Rao lower bound to check whether the unbiased MLE was UMVUE or not. Then we have:

$$ln f_X(X,\lambda) = -ln x! + x ln\,\lambda - \lambda \tag{C9}$$

$$\frac{\partial(ln f_X(X,\lambda))}{\partial\lambda} = \frac{x}{\lambda} - 1 \tag{C10}$$

And

$$\frac{\partial^2 ln f_X(X,\lambda)}{\partial\lambda^2} = \frac{\partial(\frac{x}{\lambda} - 1)}{\lambda} = -\frac{x}{\lambda^2} \tag{C11}$$

Accordingly the expectation of equation (C11) when the population parameter λ is true:

$$E_\lambda\left[\frac{\partial^2 ln f_X(X,\lambda)}{\partial\lambda^2}\right] = E_\lambda\left(-\frac{X}{\lambda^2}\right) = -\frac{1}{\lambda^2}E_\lambda(X) = -\frac{\lambda}{\lambda^2} = -\frac{1}{\lambda} \tag{C12}$$

So the Cramer-Rao lower bound (CRLB) is

$$\mathrm{CRLB} = \frac{1}{-nE_\lambda\left[\frac{\partial^2 ln f_X(X,\lambda)}{\partial\lambda^2}\right]} = \frac{1}{-n\cdot(-\frac{1}{\lambda})} = \frac{\lambda}{n} = Var_\lambda(\hat{\lambda}) = Var_\lambda(\overline{\mathrm{X}}) \tag{C13}$$

Consequently, MLE $\hat{\lambda} = \overline{\mathrm{X}}$ is UMVUE of population parameter λ.

Hydrol. Earth Syst. Sci. Discuss., doi:10.5194/hess-2016-386, 2016
Manuscript under review for journal Hydrol. Earth Syst. Sci.
Published: 1 August 2016

Figure captions

Figure 1
Description of the study area, (a) Location of the Yangjuangou Catchment; (b) restoration vegetation types at the runoff-plot scale, from left to right: *Armeniaca sibirica* (T1), *Spiraea pubescens* (T2), and *Artemisia copria* (T3); (c) field saturated conductivity measurement using Model 2800 K1 Guelph Permeameter; (d) a 1 m^2 quadrat to measure vegetation coverage

Figure 2
Construction process of OCIRS-Bayes analysis framework, (a) flow chart of confirming process of all elements in OCIRS-Bayes system; (b) Venn diagram of the relationships of all elements in OCIRS-Bayes system; (c) result of hierarchical cluster analysis of 130 individual rainfall events

Figure 3
The probability distributions of four rainfall event types at month and seasonal scales over five rainy seasons

Figure 4
The probability distributions of soil erosion in three restoration vegetation types at month and seasonal scales over five rainy seasons, the Arabic numbers and letter "T" on the abscissa in each plot represent the month and total reason respectively, the same as follow figures

Figure 5
The distribution of probabilistic contribution of four rainfall event types on one stochastic soil erosion in three restoration vegetation types at month and seasonal scales over five rainy seasons

Figure 6
The comparison the prediction of stochasticity of soil erosion by binomial and Poisson PMFs and observed frequency of numbers of times of soil erosion event in three restoration vegetation types, Exp_B and Exp_P means the expected values in binomial and Poisson PMF respectively, and histogram represents observed value.

Figure 7
Morphological structure properties of thee restoration vegetation types including litter layer, root system distribution. The diameter and depth of samples which were indicted by the dashed line are approximately 10 cm and 30 cm respectively

Hydrol. Earth Syst. Sci. Discuss., doi:10.5194/hess-2016-386, 2016
Manuscript under review for journal Hydrol. Earth Syst. Sci.
Published: 1 August 2016

Hydrology and Earth System Sciences
Open Access
Discussions

Acknowledgment

This work was funded by the National Natural Science Foundation of China (No. 41390464 and 41471094). We also thank Prof. Chen Lin-An with National Chiao Tung University (NCTU) for his great help on the mathematical statistical inference in manuscript.

Reference

Bautista, S., Mayor, A. G., Bourakhouadar, J., and Bellot, J.: Plant spatial pattern predicts hillslope runoff and erosion in a semiarid Mediterranean landscape, Ecosystems, 10, 987-998, 2007.

Bhunya, P. K., Berndtsson, R., Ojha, C. S. P., and Mishra, S. K.: Suitability of Gamma, Chi-square, Weibull, and Beta distributions as synthetic unit hydrographs, Journal of Hydrology, 334, 28-38, 2007.

Boix-Fayos, C., Martinez-Mena, M., Arnau-Rosalen, E., Calvo-Cases, A., Castillo, V., and Albaladejo, J.: Measuring soil erosion by field plots: Understanding the sources of variation., Earth-Science Reviews, 78, 267-285, 10.1016/j.earscirev.2006.05.005, 2006.

Boix-Fayos, C., Martinez-Mena, M., Calvo-Cases, A., Arnau-Rosalen, E., Albaladejo, J., and Castillo, V.: Causes and underlying processes of measurement variability in field erosion plots in Mediterranean conditions, Earth Surface Processes and Landforms, 32, 2007.

Bonham, C.: Measurements for Terrestrial Vegetation, second ed., John Wiley & Sons. Ltd, 1989.

Cammerraat, L. H.: A review of two strongly contrasting geomorphological systems within the context of scale, Earth Surface Processes and Landforms, 27, 1201-1222, 2002.

Cao, S. X., Chen, L., and Yu, X. X.: Impact of China's Grain for Green Project on the landscape of vulnerable arid and semi-arid agricultural regions: a case study in northern Shaanxi Province, Journal of Applied Ecology, 46, 536-543, 2009.

Eagleson, P. S.: Climate, soil and vegetation 2.The distribution of annual precipitation derived from observed storm sequences, Water Resource Research, 14, 713-721, 1978.

FAO-UNESCO: Soil map of the world (1:5000000), Food and agriculture organiation of the Unite Nations, UNESCO, Paris, 1974.

Fu, B., Liu, Y., He, C., Zeng, Y., and Wu, B.: Assessing the soil erosion control service of ecosystems change in the Loess Plateau of China, Ecology Complexity, 8, 284-293, 10.1016/j.ecocom.2011.07.003, 2011.

Gartner, H.: Tree roots-Methodological review and new development in dating and quantifying erosive processes, Geomorphology, 86, 243-251, 2007.

Geißler, C., Kühn, P., Böhnke, M., Bruelheide, H., Shi, X., and Scholten, T.: Splash erosion potential under tree canopies in subtropical SE China, Catena, 91, 85-93, 10.1016/j.catena.2010.10.009, 2012.

Hydrol. Earth Syst. Sci. Discuss., doi:10.5194/hess-2016-386, 2016
Manuscript under review for journal Hydrol. Earth Syst. Sci.
Published: 1 August 2016

Hydrology and Earth System Sciences
Open Access
Discussions

Gyssels, G., Poesen, J., Bochet, E., and Li, Y.: Impact of plant roots on the resistance of soils to erosion by water: a review, Progress in Physical Geography, 29, 189-217, 10.1191/0309133305pp443ra, 2005.

Jiao, J., Wang, W., and Hao, X.: Precipitation and erosion characteristics of rain-storm in different pattern on Loess Plateau, journal of Arid Land Resources and Environment, 13, 34-42, 1999.

Johns, G. G.: Runoff and soil loss in a semi-arid shrub invaded poplar box (*Eucalyptus populnea*) woodland, Rangeland Journal, 5, 3-12, 1983.

Jost, G., Schume, H., Hager, H., Markart, G., and Kohl, B.: A hillslope scale comparison of tree species influence on soil moisture dynamics and runoff processes during intense rainfall, Journal of Hydrology, 420, 112-124, 2012.

Kim. J, Ivanov. V, and Fatichi, S.: Enviromental stochasticity controls soil erosion variabilty Scientific Report, 6, 10.1038/srep22065(2016), 2016.

Kumar, S., and Kushwaha, S. P. S.: Modelling soil erosion risk based on RUSLE-3D using GIS in a Shivalik sub-watershed, Journal of Earth System Science, 122, 389-398, 10.1007/s12040-013-0276-0, 2013.

Li, L., Wang, Y., and Cao, Z.: Probabilistic slope stability analysis by risk aggregation, Engineering Geology, 176, 57-65, 2014.

Liu, S.: Evaluation of the Liu model for predicting rainfall interception in forest world-wide, Hydrological Processes, 15, 2341-2360, 2001.

Liu, Y., Fu, B., Lü, Y., Wang, Z., and Gao, G.: Hydrological responses and soil erosion potential of abandoned cropland in the Loess Plateau, China, Geomorphology, 138, 404-414, 2012.

Ludwig, J. A., Wilcox, B. P., Breshears, D. D., Tongeay, D. J., and Imeson, A. C.: Vegetation pathces and runoff-erosion as interacting ecohydrological processes in semarid landscape, Ecology 86, 288-297, 2005.

Mallick, J., Alashker, Y., Mohammad, S. A.-D., Ahmed, M., and Abul Hasan, M.: Risk assessment of soil erosion in semi-arid mountainous watershed in Saudi Arabia by RUSLE model coupled with remote sensing and GIS, Geocarto International, 29, 915-940, 10.1080/10106049.2013.868044, 2014.

Marques, M. J., Bienes, R., Perez-Rodriguez, R., and Jiménez, L.: Soil degradation in central Spain due to sheet water erosion by low-intensity rainfall events, Earth Surface Processes and Landforms, 33, 414-423, 2008.

Mohammad, A. G., and Adam, M. A.: The impact of vegetative cover type on runoff and soil erosion under different land uses, Catena, 81, 97-103, 2010.

Moore, R. J.: The PDM rainfall-runoff model, Hydrology and Earth System Sciences, 11, 483-499, 2007.

Moreno-de las Heras, M., Merino-Martin, L., and Nicolau, J. M.: Effect of vegetation cover on the hydrology of reclaimed mining soils under Mediterranean-continental climate, Catena, 77, 39-47, 2009.

Moreno-de las Heras, M., Nicolau, J. M., Merino-Martin, L., and Wilcox, B. P.: Plot-scale effects on runoff and erosion along a slope degradation gradient, Water Resource Research, 46, 10.1029/2009WR007875, 2010.

Morgan, R. P. C.: A simple approach to soil loss prediction: a revised Morgan-Finney model, Catena, 44, 305-322, 2001.

Mouri, G., Minoshima, D., Golosov, V., Chalov, S., Seto, S., Yoshimura, K., Nakamura, S., and Oki,

Hydrol. Earth Syst. Sci. Discuss., doi:10.5194/hess-2016-386, 2016
Manuscript under review for journal Hydrol. Earth Syst. Sci.
Published: 1 August 2016

T.: Probability assessment of flood and sediment disasters in Japan using the Total Runoff-Integrating Pathways model, International Journal of Disaster Risk Reduction, 3, 31-43, 2013.

Munoz-Robles, C., Reid, N., Tighe, M., Biriggs, S. V., and Wilson, B.: Soil hydrological and erosional responses in patches and inter-patches in vegetation states in semi-arid Australia, Geoderma, 160, 524-534, 2011.

Portenga, E. W., and Bierman, P. R.: Understanding earth's eroding surface with 10Be, GSA Today, 21, 4-10, 2011.

Prasannakumar, V., Shiny, R., Geetha, N., and Vijith, H.: Spatial prediction of soil erosion risk by remote sensing, GIS and RUSLE approach: a case study of Siruvani river watershed in Attapady valley, Kerala, India, Environmental Earth Sciences, 64, 965-972, 10.1007/s12665-011-0913-3, 2011.

Puigdefábregas, J.: The role of vegetation patterns in structuring runoff and sediment fluxes in drylands, Earth Surface Processes and Landforms, 30, 133-147, 2005.

Robert, V. H., Joseph, W. M., and Allen, T. C.: Introdcution to Mathematical Statistics, Pearson Education, Inc., 2013.

Rodríguez-Iturbe, I., Porporato, A., Laio, F., and Roidolfi.L: Plants in water-controlled ecosystems:active role in hydrologic processes and response to water stress I. Scope and general outline, Advances in Water Resources, 24, 695-705, 2001.

Rodriguez-Iturbe, I., Porporato, A., Ridolfi, L., Isham.V., and Cox, D. R.: Probabilstic modeling of water balance at a point: the role of climate, soil and vegetation, Proc R Soc London-Serise A, 455 3789-3805, 1999.

Sidorchuk, A.: Stochastic modelling of erosion and deposition in cohesive soil Hydrological Processes, 19, 1399-1417, 2005.

Sidorchuk, A.: A third generation erosion model: the combination of probailistic and determinstic components, Geomorphology, 2009, 2-10, 2009.

Verma, P., Yeates, J., and Daly, E.: A stochastic model describing the impact of daily rainfall depth distribution on the soil water balance., Advances in Water Resources, 34, 1039-1048, 2011.

Wang, Fu, B., Piao, S., Lu, Y., Ciais, P., Ciais, P., and Wang, Y.: Reduced sediment transport in the Yellow River due to anthropogenic changes, Nature geoscience, 9, 38-41, 10.1038/ngeo2602, 2015.

Wang, P., and Tartakovsky, D. M.: Reduced complexity models for probabilistic forecasting of infiltration rates, Advance in Water Resources, 34, 375-382, 2011.

Wang, S., Fu, B. J., Gao, G. Y., Liu, Y., and Zhou, J.: Responses of soil moisture in different land cover types to rainfall events in a re-vegetation catchment area of the Loess Plateau, China, Catena, 101, 122-128, 10.1016/j.catena.2012.10.006, 2013.

Wang, X., Zhang, Y., Hu, R., Pan, Y., and Berndtsson, R.: Canopy storage capacity of xerophytic shrubs in Northwestern China, Journal of Hydrology, 454, 152-159, 2012.

Wei, W., L., C., Fu, B., Huang, Z., Wu, D., and Gui, L.: The effect of land uses and rainfall regimes on runoff and soil erosion in the semi-arid loess hilly area, China, Journal of Hydrology, 335, 247-258, 10.1016/j.jhydrol.2006.11.016, 2007.

Wischmeier, W. H., and Smith, D. D.: Predicting rainfall erosion losses: A guide to conservation planning, Agriculture handbook Number 537, United States Department of Agriculture, 1978.

Woods, S. W., and Balfour, V. N.: The effects of soil texture and ash thickness on the post-fire hydrological response from ash-covered soils, Journal of Hydrology, 393, 274-286, 2010.

Ya, L., and Chi, Y.: Rainfall-induced landslide risk at Lushan, Taiwan., Engineering Geology, 123, 113-121, 10.1016/j.enggeo.2011.03.006, 2011.

Zhou, J., Fu, B., Gao, G., Lü, N., Lü, Y., and Wang, S.: Temporal stability of surface soil moisture of different vegetation types in the Loess Plateau of China, Catena, 128, 1-15, 2015.

Zhou, J., Fu, B., Gao, G., Lü, Y., Liu, Y., Lü, N., and Wang, S.: Effects of precipitation and restoration vegetation on soil erosion in a semi-arid environment in the Loess Plateau, China, Catena, 137, 1-11, 2016.

Zhu, H., Fu, B., Wang, S., Zhu, L., Zhang, L., and Jiao, L.: Reducing soil erosion by improving community functional diversity in semi-arid grassland, Journal of Applied Ecology, 10.1111/1365-2664.12442, 2015.

Hydrol. Earth Syst. Sci. Discuss., doi:10.5194/hess-2016-386, 2016
Manuscript under review for journal Hydrol. Earth Syst. Sci.
Published: 1 August 2016

Tables

Table 1 Basic properties of soil, vegetation and erosion in different restoration vegetation types

Basic properties of different vegetation types	[h]N	Restoration vegetation types		
		Armeniaca sibirica	*Spiraea pubescens*	*Artemisia copria*
		Type 1	Type 2	Type3
Topography property				
Slope aspect	9	southwest	southwest	Southwest
Slope gradation (%)	9	≈26.8	≈26.8	≈26.8
Slope size for each (m)	9	3×10	3×10	3×10
Soil property				
[a]DBD (g cm^{-3})	30	1.28±0.08	1.16±0.12	1.23±0.10
Clay (%)	30	11.07±2.43	11.98±3.05	9.54±1.48
Silt (%)	30	26.11±1.50	25.24±3.84	26.72±2.87
Sand (%)	30	62.82±0.94	62.78±4.51	63.74±3.24
[b]Texture type		Sandy loam	Sandy loam	Sandy loam
[c]Kfc (cm min^{-1})	20	0.46±0.82(a)	2.22±0.66(b)	0.50±0.60(a)
[d]SOM (%)	30	1.28±0.63(a)	0.98±0.15(b)	0.90±0.09(b)
Vegetation property				
Restoration years	9	20	20	20
Crown diameters (cm)	27	211.6±15.4(c)	80.5±4.5(b)	64.1±6.3(a)
Litter layer (cm)	30	1.2±0.3(a)	3.4±1.8(b)	1.8±0.5(a)
Height (cm)	27	256.3±11.1(c)	128.3±8.3(b)	61.8±1.1(a)
LAI	27	×	2.31	1.78
[e]Ave. Coverage (%)	27	85	90	90
Rainfall/Erosion property				
Times of rainfall events			130	
Times of runoff events		30/30/30	45/45/45	45/45/45
Times of sediment events		13/13/13	19/19/19	32/32/32
[f]Ave. runoff depth (cm)		0.012(a)	0.014(a)	0.083(b)
[g]Ave. sediment amount (g)		5.8(a)	6.8(a)	25.7(b)

a: dry bulk density; b: texture type is determined by textural triangle method based on USDA; c: field saturated hydraulic conductivity, and all the values with same letter in each row indicates non-significant difference at α=0.05 which is the same as follow rows; d: soil organic matter; e: average coverage of three restoration vegetation types over five rainy seasons; f: average runoff depth in restoration types over rainy seasons; g: average sediment yield in restoration types over rainy seasons; h: sample number.

Hydrol. Earth Syst. Sci. Discuss., doi:10.5194/hess-2016-386, 2016
Manuscript under review for journal Hydrol. Earth Syst. Sci.
Published: 1 August 2016

Table 2 Definition and explanation of all elements in OCIRS systems based on rainfall-erosion stochasticity framework

Type	Physical characteristic	Probabilistic characteristics	Reoccurrences and implication
O	observation event including non-rainfall and rainfall events	random events composing the sample space of OCIRS system, the probability $P(O) = 1$	indicating general stochasticity of weather conditions over rainy seasons
C	non-rainfall events including sunny or cloudy weather conditions	random events, the probability of C events is the ratio of times of C events to O events over observation, $C \subset O, 0 \le P(C) \le P(O) = 1$	implying the extent of potential evapotranspiration in weather condition
I	an individual rainfall event with different precipitation, intensity and duration ranging from 0 to 72 hours, the time interval between two I events is more than 6 hours	random events, the probability of I event is ratio of times of I events to O events over observation $I \subset O, I \cup C = O, I \cap C = \emptyset, 0 \le P(I) \le P(O) = 1$	a driven force of erosion, which could be intercepted by vegetation and have high reoccurrences in rainy season
I_A	a classified rainfall event with average precipitation and intensity being 5 mm and 0.015 mm/min respectively	random events composing the subset of I events, $I_A \subseteq I, 0 \le P(I_A) \le P(I)$	having lowest rainfall erosivity nearly triggering no soil erosion events, and highest reoccurrences in all I events
I_B	a classified rainfall event with average precipitation and intensity being 27.6 mm and 0.072 mm/min respectively	random events composing the subset of I events$I_B \subseteq I$, $I_B \cap I_A = \emptyset, 0 \le P(I_B) \le P(I_A) \le P(I)$	having middle rainfall erosivity generally triggering runoff events, and middle reoccurrences in all I events
I_C	a classified rainfall event with average precipitation and intensity being 70 mm and 0.062 mm/min respectively	random events composing the subset of I events,$I_C \subseteq I$, $I_C \cap I_B \cap I_A = \emptyset, 0 \le P(I_C) \le P(I_B) \le P(I_A) \le P(I)$	having high rainfall erosivity almost driving runoff and sediment events, and low reoccurrences in all I events

I_D	an extreme rainfall event with precipitation and intensity being 4.6 mm and 0.78 mm/min respectively	random events composing the subset of I events, $I_D \subseteq I$, $I_D \cap I_C \cap I_B \cap I_A = \emptyset, 0 \le P(I_D) \le P(I_C) \le P(I_B) \le P(I_A) \le P(I)$	having extreme rainfall erosivity to soil erosion, lowest reoccurrences in all I events
R	runoff event generating on restoration vegetation types, it occurs on rainfall processes, its duration is negligible	random events responding to I events, $R \subset I, R \cap C = \emptyset, 0 \le P(R) < P(I)$	having different reoccurrences depending on rainfall and vegetation
S	sediment event occurring on vegetation types, it occurs on runoff processes, duration is negligible	random events responding to R events, $S \subset R \subset I, S \cap C = \emptyset, 0 \le P(S) \le P(R) < P(I)$	having different reoccurrences depending on rainfall and vegetation

Table 3 Basic properties of classified types of rainfall and their effect on runoff and sediment events distribution in different restoration vegetation types

Rainfall events	Events number	Precipitation (mm)		Intensity (mm/min)		Duration (min)		Runoff events distribution			Sediment events distribution		
		Mean	[a]SD	Mean	SD	Mean	SD	[c]T1	T2	T3	T1	T2	T3
I_A	94	5.0	5.5	0.015	0.016	365.4	313.0	1	9	10	0	0	6
I_B	26	27.6	12.5	0.072	0.050	668.5	629.9	19	26	25	5	10	18
I_C	9	69.0	11.7	0.062	0.033	1597.8	1214.3	9	9	9	7	8	8
I_D	1	4.6	[b]NA	0.779	NA	5.9	NA	1	1	1	1	1	1
Total	130							30	45	45	13	19	33

a: Standard deviation; b: not applicable, the same below; c:vegetation type

Hydrol. Earth Syst. Sci. Discuss., doi:10.5194/hess-2016-386, 2016
Manuscript under review for journal Hydrol. Earth Syst. Sci.
Published: 1 August 2016

Table 4 Correlation analysis between vegetation coverage and stochasticity of runoff and sediment events

[a]Vegetation types	Runoff Events			Sediment Events		
	Probability	Expectation	Variation	Probability	Expectation	Variation
			I_A Type			
Type 1	NA	NA	NA	NA	NA	NA
Type 2	-0.61	-0.57	-0.63	NA	NA	NA
Type 3	-0.32	-0.50	-0.18	NA	NA	NA
			I_B Type			
Type 1	-0.74*	-0.48	-0.82*	NA	NA	NA
Type 2	-0.51	-0.94*	-0.78*	-0.70*	-0.60	-0.54
Type 3	-0.88*	-0.80*	0.20	-0.81*	-0.63	-0.41
			I_C Type			
Type 1	NA	NA	NA	NA	NA	NA
Type 2	NA	NA	NA	NA	NA	NA
Type 3	NA	NA	NA	NA	NA	NA
			All Types			
Type 1	-0.28	-0.32	-0.36	NA	NA	NA
Type 2	-0.13	-0.61	[b]-0.77*	-0.33	-0.58	-0.42
Type 3	-0.09	-0.36	-0.23	-0.36	-0.69	-0.33

a: vegetation coverage; b: * means significant at α=0.05

Hydrol. Earth Syst. Sci. Discuss., doi:10.5194/hess-2016-386, 2016
Manuscript under review for journal Hydrol. Earth Syst. Sci.
Published: 1 August 2016

Hydrology and Earth System Sciences
Open Access
Discussions

Figures

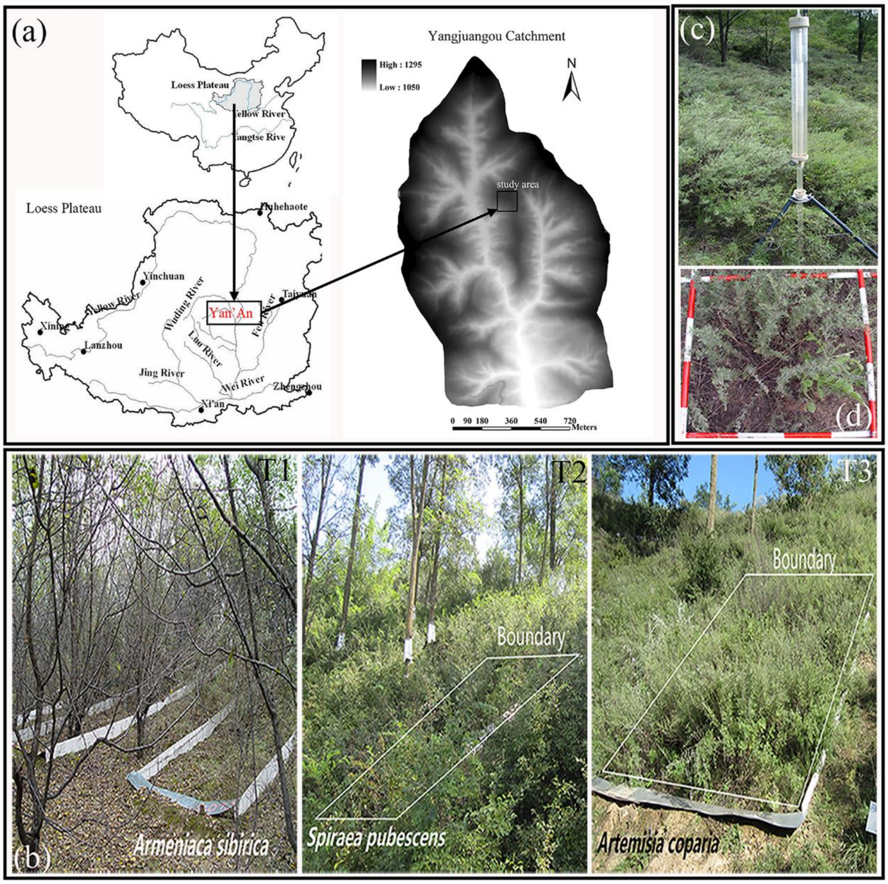

Figure 1 Description of the study area, (a) Location of the Yangjuangou Catchment; (b) restoration vegetation types at the runoff-plot scale, from left to right: *Armeniaca sibirica* (T1), *Spiraea pubescens* (T2), and *Artemisia copria* (T3); (c) field saturated conductivity measurement using Model 2800 K1 Guelph Permeameter; (d) a 1 m^2 quadrat to measure vegetation coverage

Hydrol. Earth Syst. Sci. Discuss., doi:10.5194/hess-2016-386, 2016
Manuscript under review for journal Hydrol. Earth Syst. Sci.
Published: 1 August 2016

Hydrology and Earth System Sciences
Discussions
Open Access

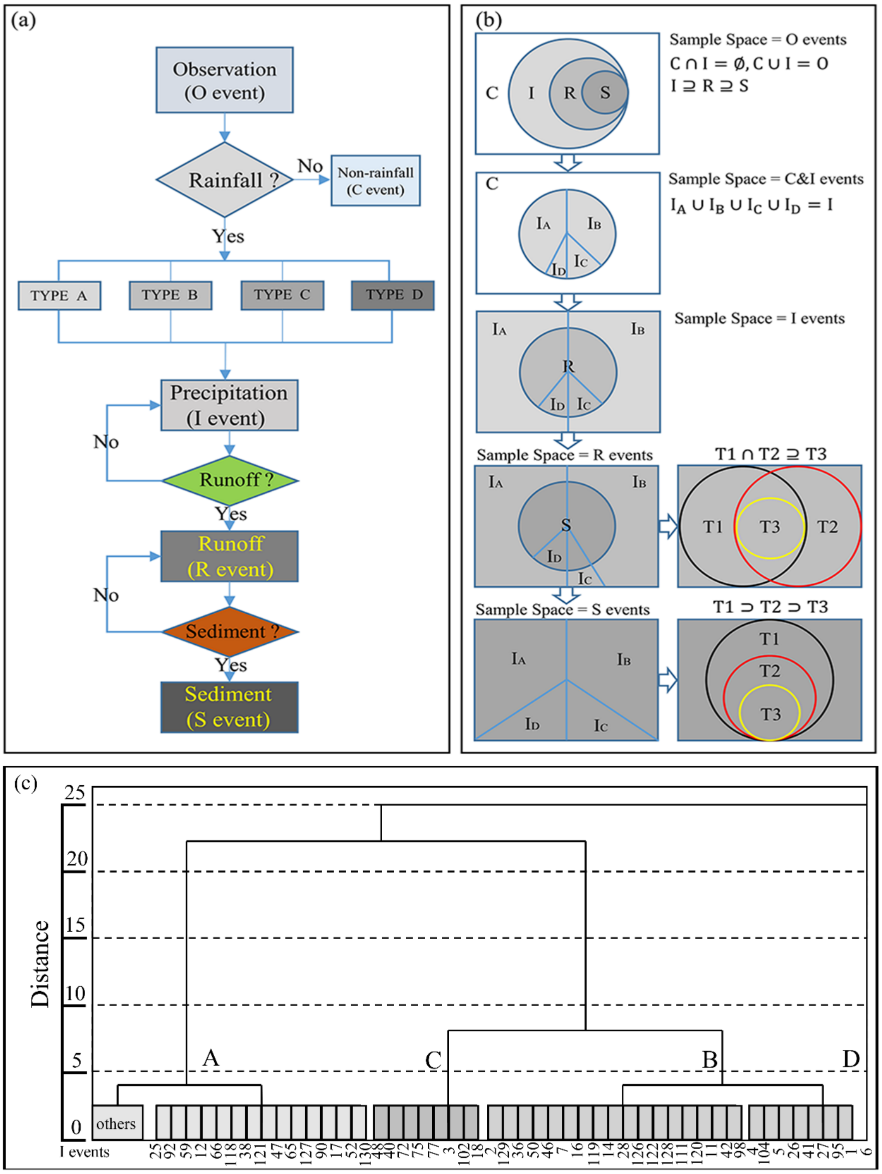

Figure 2 Construction process of OCIRS-Bayes analysis framework, (a) flow chart of confirming process of all elements in OCIRS-Bayes system; (b) Venn diagram of the relationships of all elements in OCIRS-Bayes system; (c) result of hierarchical cluster analysis of 130 individual rainfall events

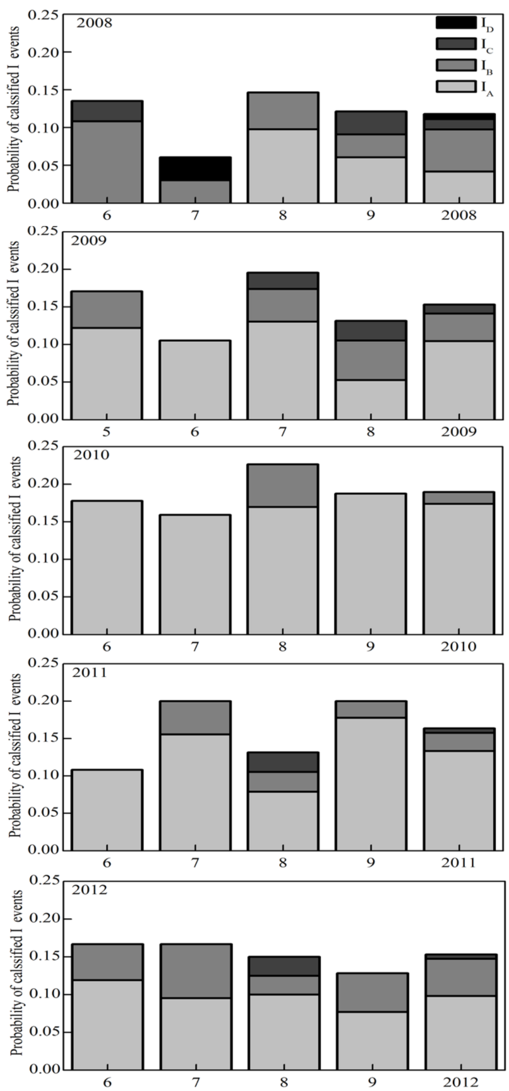

Figure 3 The probability distributions of four rainfall event types at month and seasonal scales over five rainy seasons

Hydrol. Earth Syst. Sci. Discuss., doi:10.5194/hess-2016-386, 2016
Manuscript under review for journal Hydrol. Earth Syst. Sci.
Published: 1 August 2016

Hydrology and Earth System Sciences
Discussions

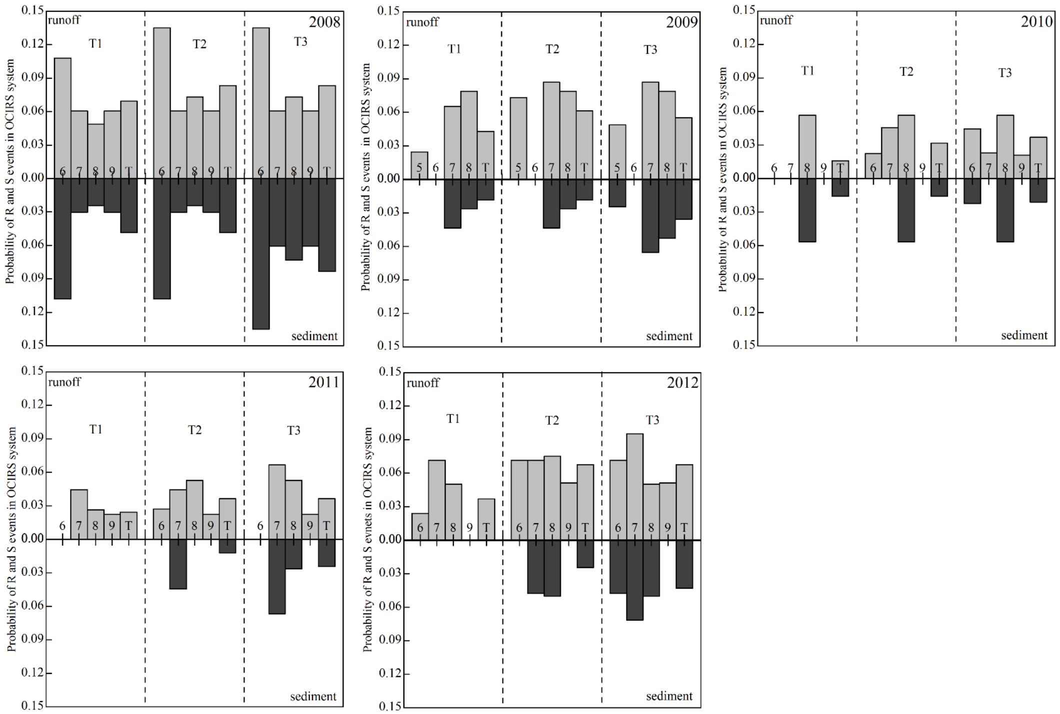

Figure 4 The probability distributions of soil erosion in three restoration vegetation types at month and seasonal scales over five rainy seasons, the Arabic numbers and letter “T” on the abscissa in each plot represent the month and total reason respectively, the same as follow figures

Figure 5

Hydrol. Earth Syst. Sci. Discuss., doi:10.5194/hess-2016-386, 2016
Manuscript under review for journal Hydrol. Earth Syst. Sci.
Published: 1 August 2016

Hydrology and Earth System Sciences
Open Access
Discussions

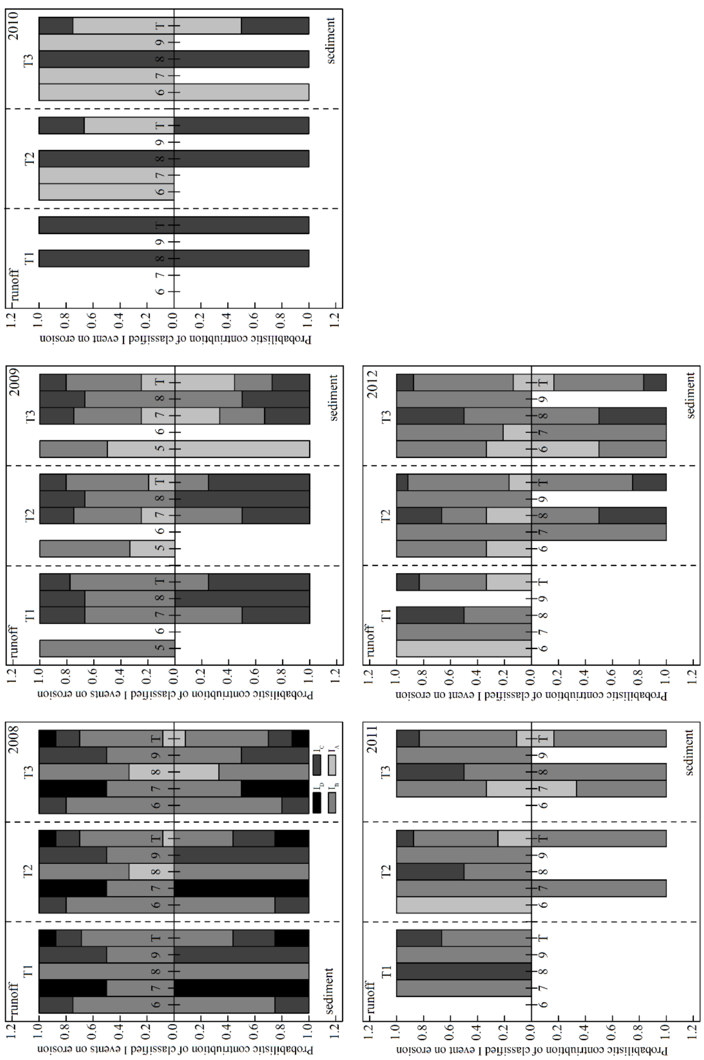

Figure 5 The distribution of probabilistic contribution of four rainfall event types on one stochastic soil erosion in three restoration vegetation types at month and seasonal scales over five rainy seasons

Hydrol. Earth Syst. Sci. Discuss., doi:10.5194/hess-2016-386, 2016
Manuscript under review for journal Hydrol. Earth Syst. Sci.
Published: 1 August 2016

Hydrology and Earth System Sciences
Open Access
Discussions

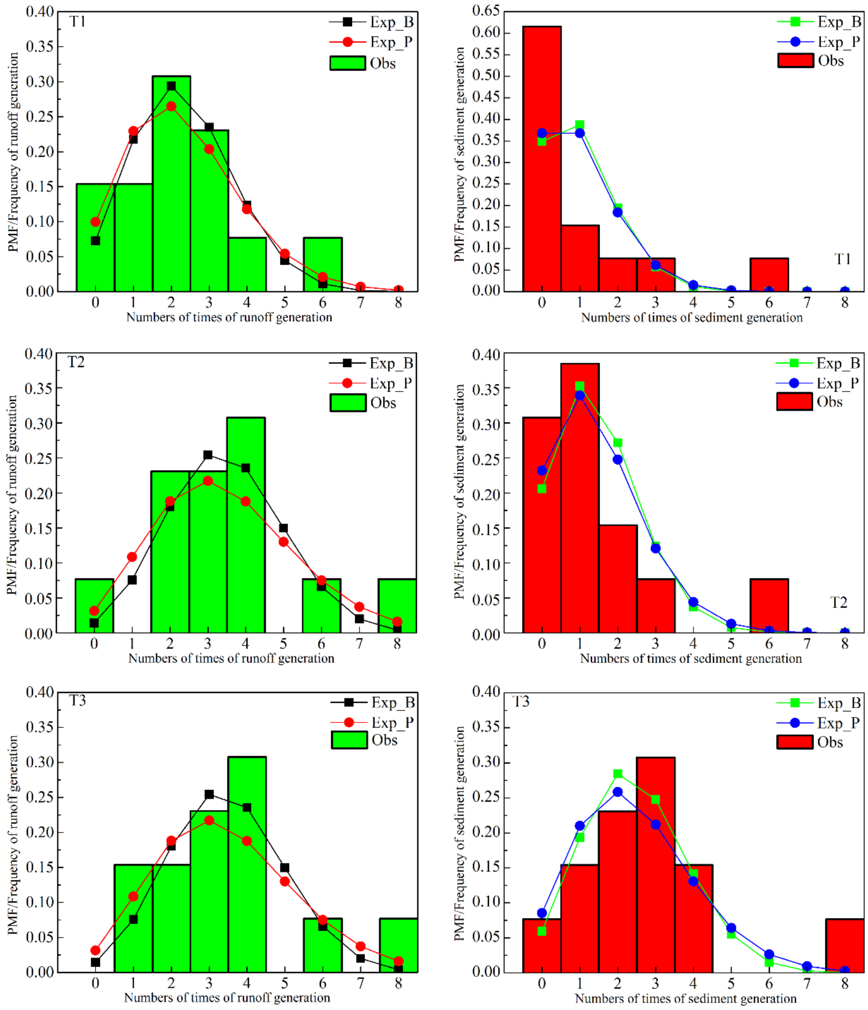

Figure 6 The comparison the prediction of stochasticity of soil erosion by binomial and Poisson PMFs and observed frequency of numbers of times of soil erosion event in three restoration vegetation types, Exp_B and Exp_P means the expected values in binomial and Poisson PMF respectively, and histogram represents observed value.

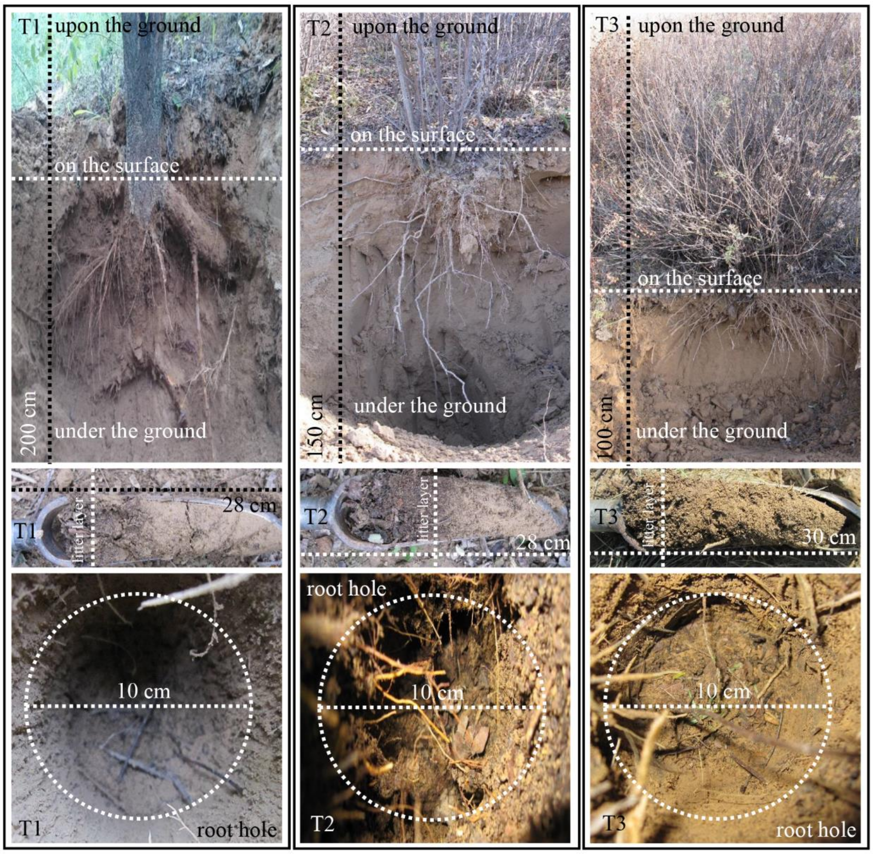

Figure 7 Morphological structure properties of thee restoration vegetation types including litter layer, root system distribution. The diameter and depth of samples which were indicted by the dashed line are approximately 10 cm and 30 cm respectively